High quality transparent TiO_2/Ag/TiO_2 composite electrode films deposited on flexible substrate at room temperature by sputtering

Aritra Dhar and T. L. Alford'

Citation: APL Materials **1**, 012102 (2013); doi: 10.1063/1.4808438
View online: http://dx.doi.org/10.1063/1.4808438
View Table of Contents: http://aip.scitation.org/toc/apm/1/1
Published by the American Institute of Physics

High quality transparent TiO_2/Ag/TiO_2 composite electrode films deposited on flexible substrate at room temperature by sputtering

Aritra Dhar[1] and T. L. Alford[1,2,a]
[1]*Department of Chemistry and Biochemistry, Arizona State University, Tempe, Arizona 85287, USA*
[2]*School for Engineering of Matter, Transport, and Energy, Arizona State University, Tempe, Arizona 85287, USA*

(Received 20 February 2013; accepted 16 April 2013; published online 7 June 2013)

Multilayer structures of TiO_2/Ag/TiO_2 have been deposited onto flexible substrates by room temperature sputtering to develop indium-free transparent composite electrodes. The effect of Ag thicknesses on optical and electrical properties and the mechanism of conduction have been discussed. The critical thickness (t_c) of Ag mid-layer to form a continuous conducting layer is 9.5 nm and the multilayer has been optimized to obtain a sheet resistance of 5.7 Ω/sq and an average optical transmittance of 90% at 590 nm. The Haacke figure of merit (FOM) for t_c has one of the highest FOMs with 61.4×10^{-3} Ω^{-1}/sq. [http://dx.doi.org/10.1063/1.4808438]

Flexible thin films of transparent conducting oxide (TCO) are extensively used for a variety of applications in optoelectronic industry, such as solar cells, electrochromic devices, liquid crystal displays, and organic light emitting diodes.[1–4] The introduction of a room-temperature route for deposition of highly conductive and transparent material onto flexible substrates could change the future of several photonic and electronic devices with the potential to influence a wide spectrum of applications.[1–3] Until now, amorphous indium tin oxide (a-ITO) has been commonly used as transparent electrode for flexible optoelectronic applications due to its low resistivity ($\sim 10^{-4}$ Ω cm) and high transmittance (~80%) in the visible region.[5] However, a-ITO film deposited on flexible substrates has some limitations such as fairly lower conductivity owing to low process temperature and reduced dopant activation at lower temperatures. The reduction in thickness of the electrode material to attain better mechanical flexibility also results in the poor conductivity problem. Indium is also a rare and highly expensive metal and thus makes the resulting fabrication costs excessive for future applications. Thus, these factors have attracted a sufficient amount of attention in search for cheaper materials with good opto-electrical properties. Promising alternative materials include pure SnO_2, ZnO, or ZnO doped with metals (i.e., aluminum (Al), gallium (Ga), etc.), Nb_2O_5, TiO_2, graphene, and carbon nanotube (CNT) sheets have been recently studied as potential alternatives to a-ITO electrodes on flexible substrates.[5–9] Recently, insertions of a very thin metal layer sandwiched between the two TCO layers have been studied to develop a transparent composite electrode (TCE) with the desired electrical conductivity.[9–12] Although metals have high reflectivity, very thin films (<15 nm) show moderate transmittance in the visible region and the top dielectric layer helps to obtain a higher transparent effect by diminishing the reflection from the metal layer. These oxide/metal/oxide (OMO) multilayers are more efficient than a single-layer TCO film.[7–13]

Titanium dioxide (TiO_2) is a potential semiconductor material with wide band gap (~3 eV) and good adhesion to the glass and plastic substrates.[14,15] It has many excellent physical properties such as a high dielectric constant and a strong mechanical and chemical stability.[16] Due to its high refractive index of about 2.7 and optical transmittance of above 90% in the visible range, TiO_2

[a]Author to whom correspondence should be addressed. Electronic mail: TA@asu.edu

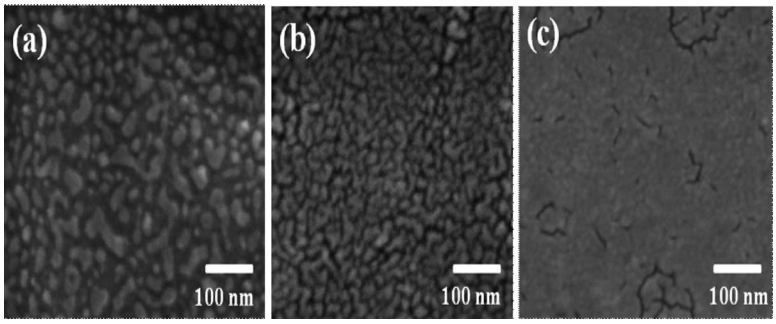

FIG. 1. SEM images of Ag thin film deposited on bottom TiO_2 surface with different Ag thicknesses: (a) 5 nm, (b) 9.5 nm, and (c) 13 nm.

can be used as optical coatings on large area substrates for architectural, automotive and display applications and protective layers for very large-scale integrated circuits.[14–16] In this work, the high transparency of TiO_2 in visible region and low resistivity of thin Ag layer lead us to the detailed study of optical and electrical properties of TiO_2/Ag/TiO_2 (TAT) multilayer as TCEs. The multilayer transparent conductive electrodes have been deposited onto flexible substrates by sputtering at room temperature. The performance of this system based on the optical and electrical properties has been evaluated using a figure of merit (FOM).

The TiO_2/Ag/TiO_2 multilayer thin films of different silver thicknesses were sequentially deposited onto 125 μm thick flexible polyethylene naphthalate (PEN) and Si substrates by rf magnetron sputtering of ceramic TiO_2 target (99.999% purity) and dc sputtering of pure Ag target (99.99% purity) at room temperature without any vacuum break. The TiO_2 and Ag were deposited using rf power and dc power of 150 W and 40 W, respectively. Bare TiO_2 layers were also deposited under identical conditions on PEN to compare the physical properties. The top and bottom TiO_2 layers were approximately 30 nm thick; while, the silver thickness was varied between 5 and 13 nm. The thicknesses of the TAT multilayer films were determined using optical ellipsometry. Scanning electron microscope (XL30 ESEM, Philips) at an operating voltage of 20 kV was used to analyze the surface morphology of different thicknesses of Ag layers grown on the bottom TiO_2 layer. Hall measurements by the van der Pauw technique with a magnetic field of 0.98 T were done using the Ecopia HMS 3000 instrument. Four-point-probe technique was used for sheet resistance measurements. Optical transmittance of the multilayers was measured using an Ocean Optics double channel spectrometer (model DS200) in the wavelength range of 300–800 nm with an air reference for transmittance. Deuterium and tungsten halogen lamps were used as sources for UV and visible light, respectively.

A systematic study is done in order to determine the effect of Ag mid-layer on the opto-electrical properties of multilayer thin films. The most vital factor that influences the performance of the composite is the morphology of the middle metal layer. It is known that the Ag film growing on an amorphous TiO_2 surface should follow the island growth mechanism of Volmer-Weber model[17,18] which is verified from the microstructure in Fig. 1. The SEM images correspond to different Ag thicknesses before and after the critical thickness of 9.5 nm. Figure 1(a) shows the presence of island structures which gradually form contiguous layer as it approaches the critical thickness [Fig. 1(b)]. Finally, the Ag islands form a continuous layer [Fig. 1(c)] at 13 nm. In order to achieve high transmittance in the visible region, the thickness of the Ag layer is limited to an optimum thickness so that the TAT multilayers exhibit high conductivity as well as transparency.

Figure 2 shows the change in carrier concentration and Hall mobility as a function of Ag thickness for various TAT multilayers. The plot indicates that carrier concentration depends strongly on the Ag thickness. The carrier concentration of the TAT multilayer has increased from 6.8×10^{21} to 1.46×10^{22} cm^{-3} upon increase in Ag thickness from 5 to 13 nm. Hence, metallic conduction is dominant in this TAT system. There is a rapid increase in Hall mobility that occurs with increasing Ag layer thickness from 3.7 cm^2/V-s at 5 nm to 13.1 cm^2/V-s at 13 nm, respectively. There are many

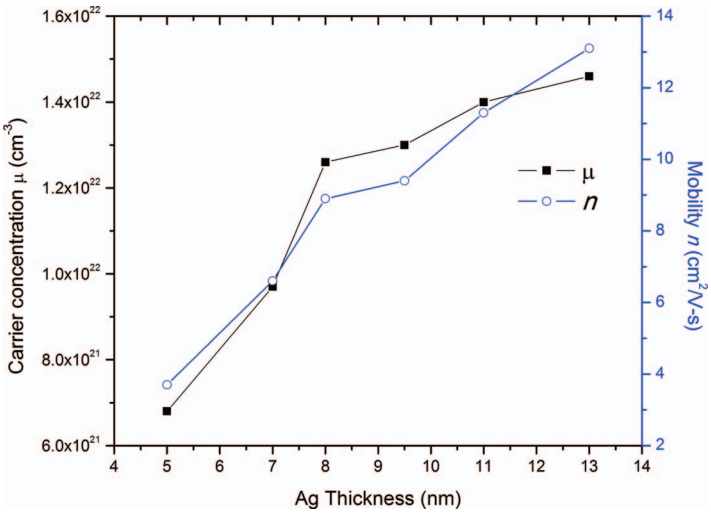

FIG. 2. Carrier concentration and Hall mobility as a function of Ag thickness for TAT multilayers.

scattering mechanisms such as phonon scattering, grain-boundary scattering, surface scattering, interface scattering, and ionized-impurity scattering.[7,9] Since TiO_2 is an amorphous and intrinsic semiconductor, one can exclude the possibility of ionized-impurity scattering. In our TCE, interface scattering takes place above the critical thickness of 9.5 nm; whereas island boundary scattering dominates at the TiO_2/Ag interface below the critical thickness due to the presence of Ag island structures. These boundaries are expected to have fairly high densities of interface states which scatter free carriers due to the presence of trapped charges and inherent disorders. As a result, a space charge region is created in the island boundaries, which results in potential barriers to charge transport due to band bending. This transport phenomenon in polycrystalline thin films can be expressed by Petritz model,[19] where the mobility (μ_i) is written as

$$\mu_i = \mu_0 \exp(-\frac{\Phi_B}{k_B T}), \tag{1}$$

where $\mu_0 = (\frac{S^2 e^2}{2\pi m^* k_B T})^{\frac{1}{2}}$.

S is the island size, e is the elementary charge, Φ_B is the island boundary potential, and k_B is the Boltzmann constant.

Figure 3 shows the effect of Ag mid-layer on the resistivity and sheet resistance of TAT multilayers where both decrease with increasing thickness of the Ag mid-layer in the multilayer. In this case, TiO_2 is an insulator with resistivity of the order of 10^7 Ω cm. On depositing a 5 nm Ag film between the TiO_2 layers, the resistivity decreases to 8.8×10^{-4} Ω cm and suggests that there is a 11-fold decrease in resistivity in TAT multilayers when compared to bare TiO_2. As the Ag thickness is increased from 5 nm to 13 nm, the effective resistivity gradually decreases down to 4.45×10^{-5} Ω cm. A more detailed investigation of Fig. 2 shows that the effective resistivity of the TAT multilayers drops significantly from 5 to 7 nm and indicates the presence of small Ag island structures in case of 5 nm deposition. However, there is a slow decrease in the effective resistivity of the multilayers from 7 to 13 nm with TAT multilayers approaching the resistivity of bulk silver. The change in effective resistivity of the TAT multilayer films with increasing Ag thickness can be explained using the following basic relation:

$$\rho_{eff} = \frac{1}{ne\mu}. \tag{2}$$

The sheet resistance curve follows similar trend to that of resistivity as a function of Ag thickness achieving data close to bulk Ag on 13 nm thickness. Here also, we see a rapid decrease in sheet resistance from 50.6 Ω/sq to 5.5 Ω/sq as the mid-Ag layer increases from 5 to 9.5 nm. However,

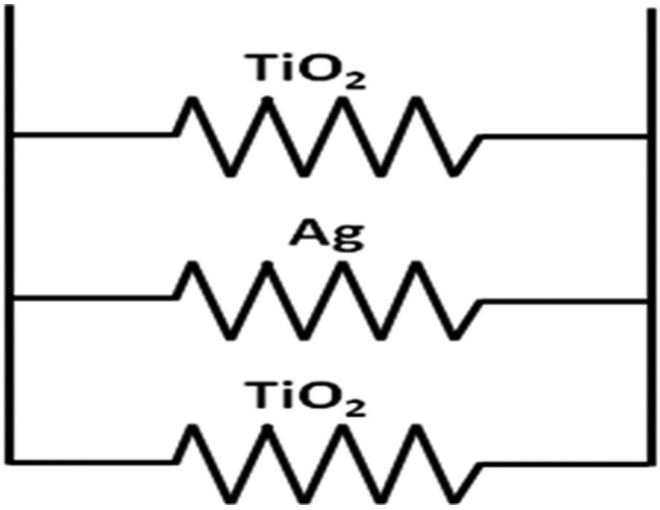

FIG. 3. Schematic diagram of parallel resistor in TAT multilayer electrode.

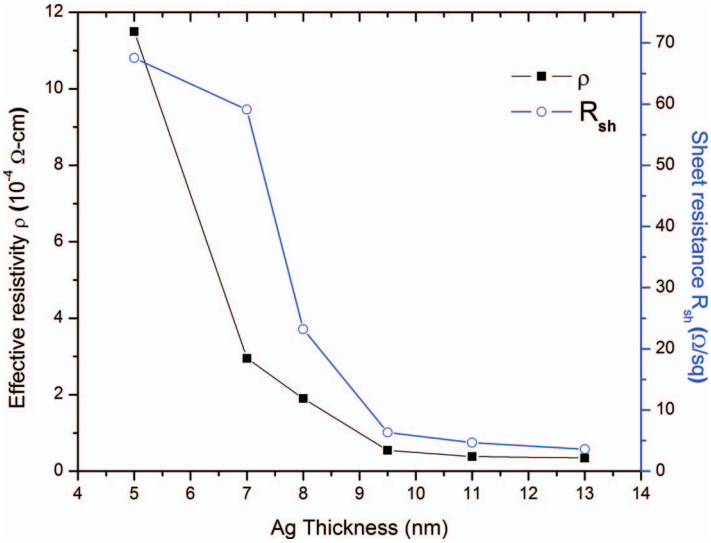

FIG. 4. Effective resistivity and sheet resistance of TAT multilayer films as a function of Ag thickness.

the total resistance of the TAT multilayer is a result of parallel combination of the three individual layers of TiO_2/Ag/TiO_2 and is shown in Fig. 3.

Figure 4 shows the effect of Ag mid-layer on the effective resistivity and sheet resistance of the TAT multilayers where both parameters decrease with increasing thickness of the Ag mid-layer. From the microstructure of the Ag thin film, it is clear that the Ag film deposited was discontinuous below the critical thickness (t_c) and gradually became continuous after t_c. Hence we expect different conduction mechanism before and after critical thickness.

Conduction through the dielectric dominates when the metal islands are very small and space between islands is large. As the islands grow, the separation between the islands decreases and some of the islands undergo coalesce in large scale.[20] This leads to a radical drop in resistance as observed in lower thickness region of Fig. 4. Quantum tunneling occurs between the larger islands with small gaps between them while bulk conduction occurs through the contiguous layer. The effective conductivity (σ) in this region is governed by the following equation:[21,22]

$$\sigma \propto \exp(-2\beta L - \frac{W}{k_B T}), \tag{3}$$

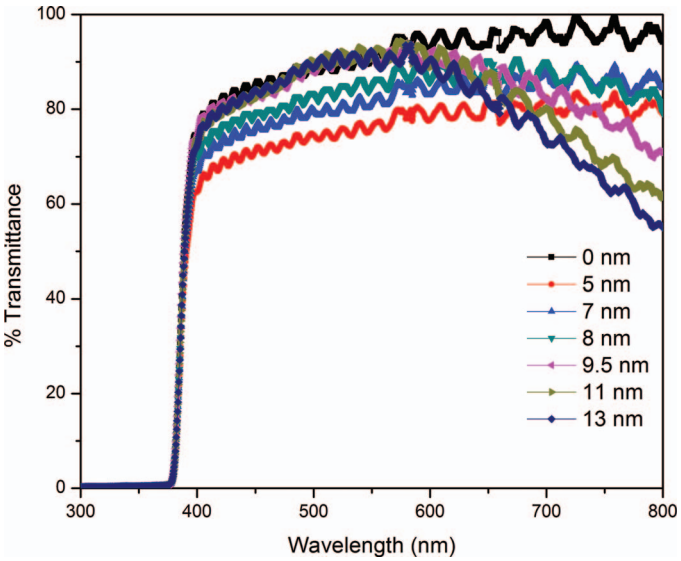

FIG. 5. Transmittance spectra for TiO_2/Ag/TiO_2 (TAT) multilayers on PEN substrate as a function of silver thickness.

where W is the island charging energy, L is the island separation, β is the tunneling exponent of electron wave functions in the insulator, k is the Boltzmann constant, and T is the temperature.

A rough surface or interface results in more diffuse scattering and thus increases resistivity of the thin film that can be either surface scattering or grain-boundary scattering. These phenomena are less prominent as the metal thickness approaches the mean free path of the conducting electrons (λ_o). Mayadas and Shatzkes[23] explained that the effect of grain boundary scattering is more predominant in polycrystalline thin films as the grain size is smaller than λ_o. When the Ag islands form a contiguous layer, the decrease in resistivity is governed by the combined effect of the increase in carrier concentration of conducting electrons and mobility. At this stage, the dominant factor affecting resistivity was surface boundary scattering. The conductivity (σ) in this region behaves according to the following equation:[21,22]

$$\frac{\sigma}{\sigma_0} \propto \frac{3}{4}(1-p)\kappa \log \frac{1}{\kappa}, \tag{4}$$

where p is the fraction of the distribution function of the electrons arriving at the surface, σ_0 represents the conductivity of the bulk metal, and $\kappa = t/\lambda_o$

Figure 5 shows optical transmittance spectra for TiO_2/Ag/TiO_2 multilayers on PEN substrate as a function of silver thicknesses. The maximum optical transmittance of the pure single-layer TiO_2 film is about 95% in the visible region. TAT multilayers show a maximum transmittance of 86% for 9.5 nm Ag thickness at ~550 nm wavelength.

It was observed that there is a parabolic increase in average optical transmittance with increasing Ag thickness and the trend is different for middle (500–600 nm) and longer wavelengths which can be explained based on scattering and absorption by the Ag mid-layer. The difference at 500–600 nm wavelength region is due to light scattering at the TiO_2/Ag interface in Ag isolated islands for Ag thickness below 8 nm and absorption of light due to interband electronic transitions from the $3d$ to unoccupied levels in the $4s$ band above Fermi level.[8,9] However, below this thickness, the transmittance decreases because the silver islands are discontinuous. In discontinuous Ag films, a size-dependent variation in the dielectric function is known to exist due to limitation of the mean free path of the conduction electrons. This leads to a correction to the imaginary part of the overall dielectric function (ε_R) given by[22]

$$\varepsilon_R = \varepsilon_m + \frac{C}{R}, \tag{5}$$

where ε_m is the dielectric constant of the bulk metal, c is a constant at a particular wavelength, and R is the particle radius. As a result, the transmittance decreases with smaller island size below the critical thickness. As the Ag thickness increases, the Ag becomes a continuous layer from discontinuous islands that causes decrease in light scattering.

In the visible region, higher transmittance was observed which can also be explained on the coupling between the incident light and surface plasmon of the island like structures of Ag thin films.[24–26] However, in the longer wavelength (700–800 nm) region the transmittance decreased abruptly for larger Ag thickness (11–13 nm), a trend similar to the optical behavior of bulk metals. In the near IR region, the increase in electron carriers results in low transmission is due to plasmon absorption dependent reflection. From the Drude-Lorentz free electron model, the plasmon frequency (ω_p) can be expressed by the following equation:[25,26]

$$\omega_p = \sqrt{\frac{ne^2}{m\varepsilon_0}}, \tag{6}$$

where n is the carrier density of electrons and ε_o is the permittivity of free space.

A figure of merit, φ_{TC} (as defined by Haacke) was estimated for each of the TAT multilayers using the following relationship:[27]

$$\varphi_{TC} = \frac{{T_{av}}^{10}}{R_{sh}}, \tag{7}$$

where T_{av} is the average transmittance and R_{sh} is the sheet resistance. The multilayer with mid-Ag thickness 9.5 nm has the best figure of merit with $61.4 \times 10^{-3}\ \Omega^{-1}$ which is one of the highest FOMs reported till date on flexible substrate at room temperature.

In conclusion, different multilayer structures of TiO_2/Ag/TiO_2 have been deposited on PEN, characterized and developed as transparent conductive film with low resistance. Hall measurements and sheet resistance data show that the conductivity of the TAT multilayer is solely due to the Ag mid-layer. The multilayer stack has been optimized to have sheet resistance of 5.7 Ω/sq and an average optical transmittance of 86% at 550 nm. The multilayer with mid-Ag thickness 9.5 nm has the best figure of merit with $61.4 \times 10^{-3}\ \Omega^{-1}$. This makes it possible to synthesize low resistivity electrode at room temperature without using high substrate temperature or post annealing process. Thus the TAT multilayers on PEN substrates can be used as transparent electrode for solar cell and other display application.

This work was partially supported by the National Science Foundation (C. Ying, Grant No. DMR-0902277) to whom the authors are greatly indebted.

[1] Q. Wan, E. N. Dattoli, and W. Lu, Appl. Phys. Lett. **90**, 222107 (2007).
[2] G. Gustafsson, Y. Cao, G. M. Treacy, F. Klavetter, N. Colaneri, and A. J. Heeger, Nature (London) **357**, 477 (1992).
[3] D. C. Look, K. D. Leedy, D. H. Tomich, and B. Bayraktaroglu, Appl. Phys. Lett. **96**, 062102 (2010).
[4] S. X. Zhang, S. Dhar, W. Yu, H. Xu, S. B. Ogale, and T. Venkatesan, Appl. Phys. Lett. **91**, 112113 (2007).
[5] V. Bhosle, A. Tiwari, and J. Narayan, Appl. Phys. Lett. **88**, 032106 (2006).
[6] K. L. Chopra, S. K. Major, and D. K. Pandya, Thin Solid Films **102**, 1 (1983).
[7] H. Han, N. D. Theodore, and T. L. Alford, J. Appl. Phys. **103**, 013708 (2008).
[8] A. Dhar and T. L. Alford, J. Appl. Phys. **112**, 103113 (2012).
[9] A. Indluru and T. L. Alford, J. Appl. Phys. **105**, 123528 (2009).
[10] T. Y. Park, Y. S. Choi, J. W. Kang, J. H. Jeong, S. J. Park, D. M. Jeon, J. W. Kim, and Y. C. Kim, Appl. Phys. Lett. **96**, 051124 (2010).
[11] C. Guillén and J. Herrero, Thin Solid Films **520**, 1 (2011).
[12] D. S. Ghosh, T. L. Chen, and V. Pruneri, Appl. Phys. Lett. **96**, 041109 (2010).
[13] K. Sivaramakrishnan and T. L. Alford, J. Appl. Phys. **106**, 063510 (2009).
[14] I. Dima, B. Popescu, F. Iova, and G. Popescu, Thin Solid Films **200**, 11 (1991).
[15] C. H. Heo, S.-B. Lee, and J.-H. Boo, Thin Solid Films **475**, 183 (2005).
[16] K. Hashimoto, H. Irie, and A. Fujhishima, Jpn. J. Appl. Phys. **44**, 8269 (2005).
[17] T. Muller and H. Nienhaus, J. Appl. Phys. **93**, 924 (2003).
[18] R. Koch, J. Phys.: Condens. Matter **6**, 9519 (1994).
[19] R. L. Petritz, Phys. Rev. **104**, 1508 (1956).
[20] K. Sivaramakrishnan and T. L. Alford, Appl. Phys. Lett. **94**, 052104 (2009).
[21] D. Zhang, H. Yabe, E. Akita, P. Wang, R. Murakami, and X. Song, J. Appl. Phys. **109**, 104318 (2011).

[22] K. Sivaramakrishnan and T. L. Alford, Appl. Phys. Lett. **96**, 201109 (2010).
[23] F. Mayadas and M. Shatzkes, Phys. Rev. B **1**, 1382 (1970).
[24] D. Zhang, P. Wang, R. Murakami, and X. Song, Appl. Phys. Lett. **96**, 233114 (2010).
[25] P. Wang, D. Zhang, D. H. Kim, Z. Qiu, L. Gao, R. Murakami, and X. Song, J. Appl. Phys. **106**, 103104 (2009).
[26] R. Doremus, Thin Solid Films **326**, 205 (1998).
[27] G. Haacke, J. Appl. Phys. **47**, 4086 (1976).